Determination of magnetic anisotropy in the LnTRENSAL complexes (Ln = Tb, Dy, Er) by torque magnetometry

Original Citation:

Determination of magnetic anisotropy in the LnTRENSAL complexes (Ln = Tb, Dy, Er) by torque magnetometry / Perfetti, Mauro; Lucaccini, Eva; Sorace, Lorenzo; Costes, Jean Pierre; Sessoli, Roberta. - In: INORGANIC CHEMISTRY. - ISSN 0020-1669. - STAMPA. - 54:(2015), pp. 3090-3092. [10.1021/acs.inorgchem.5b00288]

Published version:

DOI: 10.1021/acs.inorgchem.5b00288

Determination of magnetic anisotropy in the LnTRENSAL complexes (Ln = Tb, Dy, Er) by torque magnetometry

Mauro Perfetti [†], Eva Lucaccini[†], Lorenzo Sorace[†], J. Pierre Costes[‡] and Roberta Sessoli[†]*

[†]Dipartimento di Chimica "Ugo Schiff" and UdR INSTM, Università degli Studi di Firenze, Via della Lastruccia 3-13, 50019 Sesto Fiorentino, Italy.

[‡]Laboratoire de Chimie de Coordination 205, route de Narbonne 31077 Toulouse, Cedex 4, France.

KEYWORDS: Torque Magnetometry, Magnetic anisotropy, Lanthanides, Spin Hamiltonian, Crystal Field

Supporting Information

ABSTRACT: We report here a study about the magnetic anisotropy of the LnTRENSAL complexes (Ln=Tb, Dy, Er) using cantilever torque magnetometry and EPR. For all the compounds we extracted a set of Crystal Field parameters to obtain the energy level splitting of the ground multiplet.

Magnetic anisotropy is a fundamental property which deeply affects the magnetic behavior of molecules that exhibit slow relaxation of magnetization, called Single Molecule Magnets (SMMs).[1] Among this class of systems, a central role is played by lanthanide-based SMMs. Indeed the unquenched orbital momentum of these ions, caused by the partially filled f-orbitals interacting with the electrostatic potential originated by the ligands, is often able to give rise to huge anisotropy barriers.[2,3] The magnetic anisotropy of SMMs containing lanthanide ions (Ln) is generally rationalized by modeling the effect of the ligands using approximate point charge distributions:[4-7] however deceptive results can be obtained, especially in low-symmetry compounds.[8,9] The correlation between magnetic anisotropy and magnetization dynamics is also not always straightforward, as recently shown for two isostructural compounds containing a central Er^{3+} or Dy^{3+} ion surrounded by the trianion of the heptadentate ligand 2,2',2''-Tris(salicylideneimino)triethylamine (H_3TRENSAL).[10] The LnTRENSAL family has been extensively studied in literature both to develop new synthetic strategies,[11,12] to investigate interaction with surfaces,[13] and to study the energy pattern and thus obtain the set of the Crystal Field (CF) parameters *via* magnetic[14] and luminescence[15,16] measurements.

Cantilever Torque Magnetometry (CTM) is a powerful tool to investigate magnetic anisotropy on single crystals of lanthanide complexes in a wide temperature range.[17,18] In this work we have employed this technique to characterize in detail the magnetic anisotropy of LnTRENSAL (Ln = Tb, Dy and Er, hereafter **Tb**, **Dy**, and **Er**, respectively).

In CTM a sample is fixed on the cantilever acting as the upper plate of a capacitor.[19,20] The whole system can be rotated in an external magnetic field (**B**) and the magnetic torque ($\boldsymbol{\tau}$) experienced by the sample is directly proportional to the cantilever deflection detected as the change in the electric capacitance.

Hexagonally shaped single crystals belonging to the trigonal P-3c1 (n. 163) space group were grown for the three compounds as previously described.[10,11] The lanthanide ion lies on a special position (C_3 symmetry) thus all molecules are isooriented. Crystals faces were indexed on a single crystal diffractometer to correlate the crystallographic reference frame (*abc*) to the laboratory one (*XYZ*), where *X* corresponds to the normal to the cantilever, while the torque is measured along *Y*, i.e. the rotation axis of the cantilever (see Figs. S1-S3).

The magnetic torque is defined as the vector product between magnetization **M** and **B**.[1,19] Taking into account that experimentally only the *Y*-component of $\boldsymbol{\tau}$ can be detected, it is possible to write τ_Y as (eq 1):

$$\tau_Y = M_Z B_X - M_X B_Z = B^2 \sin\theta \cos\theta \, (\chi_{zz} - \chi_{xx}) \qquad (1)$$

where θ is the angle between **B** and the Z axis and $\boldsymbol{\chi}$ is the susceptibility tensor. The second part of eq(1) is only valid when the magnetization is linear with the applied field, that is, in general, for weak fields or high temperatures. Following eq 1, the torque signal can be considered a direct measurement of the magnetic anisotropy of the molecule. Although torque magnetometry is able to detect magnetic anisotropy contributions even when arising from magnetically inequivalent molecules,[17] and also from polynuclear clusters,[21-24] the present case is much more favorable, since the macroscopic shape of the crystals easily permits to identify the *c* crystallographic axis, which is also a molecular symmetry axis.

Two rotations have been performed: the first (rot 1) having *Y* lying in the *ab* plane, and Z coincident with –*c*, while the second (rot 2) scanning the *ab* plane, *ergo* the rotation axis was the *c* crystallographic axis (see Fig. S4).[18]

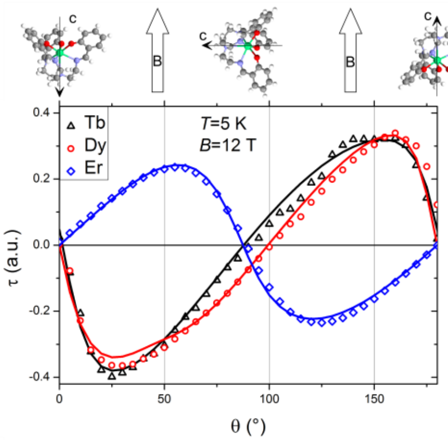

Figure 1. Torque signals for **Tb**, **Dy** and **Er** obtained at 5 K and 12 T; solid lines are the best fit curves.

In Fig. 1 we report the torque signals obtained in rot 1 for **Er**, **Dy** and **Tb** at fixed temperature (5 K) and magnetic field (12 T) (in Figs. S5-S7 all the fits are reported). The data in Fig. 1 were normalized for the different mass of the measured crystals. Beyond the trivial 180° periodicity, we first note that τ has an opposite phase for **Er** compared to **Tb** and **Dy**. According to eq 1 this means that the term ($\chi_{zz} - \chi_{xx}$)=($\chi_c - \chi_{ab}$) is positive for **Er** while is negative for **Tb** and **Dy**, testifying that different distributions of the electronic density around the lanthanide ion are mirrored in diverse anisotropy features.[8,25,26] The shape of the torque profile, with the largest $|\partial\tau/\partial\theta|$ characteristic of the hard direction, indicates that θ=0° corresponds to a hard axis for **Tb** and **Dy**, while it is an easy axis for **Er**. None of the compounds showed a detectable torque signal for measurements performed in the *ab* plane (rot2) indicating that the *ab* plane has to be considered magnetically isotropic for our sensitivity (Fig. S8). We can then conclude that the anisotropy of **Er** is easy axis, while the one of **Dy** and **Tb** is easy plane. These results are in agreement with previous powder Electron Paramagnetic Resonance (EPR) studies on **Er** and **Dy**[10] and are particularly interesting for **Tb,** a non-Kramers ion with no SMM behavior, for which the latter technique provides nonconclusive results. Indeed the powder X-band EPR spectrum of **Tb** at 5 K showed an hyperfine split transition with isotropic lineshape at about zero field, both in the perpendicular and parallel polarization mode (Figure S9).

The sensitivity of CTM allowed us to measure the angular dependence of torque at different fields even at high temperatures, where the first excited levels are also populated. These data can then be fit using an appropriate set of CF parameters. In favorable cases, like the LnTRENSAL family, a good set of CF parameters can be also obtained by luminescence measurements. However, while CTM provides direct information on the anisotropy of the ground Russell-Saunders multiplet, in luminescence spectra transitions that involve the ground multiplet may not be observed (as for **Tb** and **Dy**). In these cases the electronic structure of the ground multiplet is obtained indirectly by the set of CF parameters needed to reproduce transitions to upper lying multiplets. This may result in an incorrect prediction of the angular and field dependence of the magnetic anisotropy at low temperatures (see Fig. S10).

Parameter (cm^{-1})	**Tb**	**Dy**	**Er**
B_2^0	-562 (152)	-710 (38)	-726 (115)
B_4^0	40 (36)	-274 (80)	-81 (162)
B_6^0	-1410 (2115)	1309 (183)	952 (88)
B_4^3	1344 (520)	-1406 (98)	-2401 (233)
B_6^3	712 (498)	674 (69)	366 (69)
B'^{-3}_6	420 (420)	-760 (334)	300 (900)
B_6^6	1137 (887)	935 (187)	490 (157)
B'^{-6}_6	840 (840)	0 (-)	120 (360)

Table 1. CF parameters according to Wybourne's formalism, obtained by fitting torque signals. Numbers in brackets refer to the errors estimated by the MINUIT subroutine.

The CF Hamiltonian in Wybourne's notation for a C3 symmetry is:[27]

$$\mathcal{H}_{CF} = B_0^2\boldsymbol{C_0^2} + B_0^4\boldsymbol{C_0^4} + B_0^6\boldsymbol{C_0^6} + B_3^4\left(\boldsymbol{C_{-3}^4} - \boldsymbol{C_3^4}\right) + B_3^6\left(\boldsymbol{C_{-3}^6} - \boldsymbol{C_3^6}\right) + \mathrm{i}B'^6_3\left(\boldsymbol{C_{-3}^6} + \boldsymbol{C_3^6}\right) + B_6^6\left(\boldsymbol{C_{-6}^6} + \boldsymbol{C_6^6}\right) + \mathrm{i}B'^6_6\left(\boldsymbol{C_{-6}^6} - \boldsymbol{C_6^6}\right) \qquad (2)$$

where the *xyz* molecular reference frame was chosen to have $B'^4_3=0$ without any loss of generality.[14,15,28] All the calculations took into account the Zeeman term and the Russell-Saunders ground state, which is the only one significantly populated in the investigated temperature range.[15] The fits were performed by projecting the Hamiltonian (2) onto the ground *J* state and using the corresponding set of Stevens' extended operators. In Table 1 we reported the obtained best fit CF parameters (see also Tables S1-S2 and Eq. S1). The effective orientation of the crystals was taken into account by using two polar angles (δ=$\widehat{Zc}$; α=$\widehat{Ya}$). Due to the isotropy of the *ab* plane, α was fixed at the value obtained by the indexing, while δ was different from zero only for **Tb** (δ=0.3(1)°).

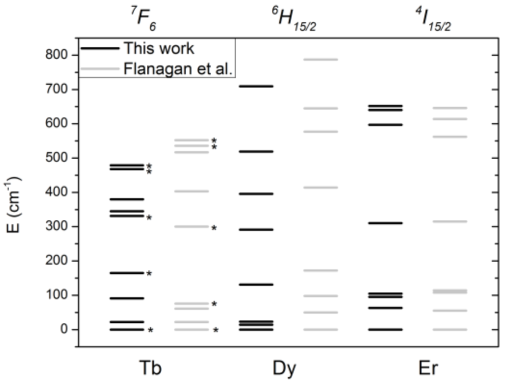

Figure 2. Energy patterns calculated using the CF parameters for the ground manifolds *J*=6, 15/2, 15/2 of **Tb**, **Dy** and **Er**, respectively, obtained by CTM (black) and luminescence (grey). All the levels are doublets, except for the ones indicated with black stars, which are singlets.

With the obtained CF parameters we calculated the energies for all the sublevels of the ground state for the three compounds and compared them with the results obtained by Flanagan *et al.* (Fig. 2).[15] The agreement between the levels calculated starting from the two techniques is particularly good for **Er,** for which luminescence provided a direct measure of the ground multiplet splitting (numerical results and details are reported in Tab. S3-S5). It is however worth noting that, due to the strong correlation between CF parameters, the uncertainty on some parameters is huge, as also occurring by using other techniques.[14,15] Interestingly, the χT vs T plot of **Tb**, **Dy** and **Er** can be simulated with comparable agreement by using our parameters and those reported by Flanagan *et al.*[15] and by Dreiser *et al.*[14](see Fig. S11). This evidences the necessity of a simple but anisotropy-sensitive technique to refine our estimation of CF parameters.[28]

The obtained results also provide an important *caveat* about the interpretation of the EPR spectra of non-Kramers' Ln ions. As already mentioned, the X-band EPR powder spectrum of **Tb** (Fig. S9) features a transition close to zero field. This is not compatible with the energy level pattern calculated using the CF parameters derived either from CTM or luminescence,[15,16] indicating a singlet ground state well separated in energy by the first excited doublet (Fig.2, Tab. S3), nor with a doublet ground state (strictly degenerate in trigonal symmetry), which may arise by a different choice of CF parameters. While a more detailed study might provide a definitive answer, we hypothesize that the observed EPR transition may be due to Tb^{3+} centers that experience a lower symmetry CF, resulting in two low-lying singlets separated by about 0.3 cm^{-1} (the microwave energy in X-band). The situation is reminiscent of what reported for $[Tb(nicotinate)_3{\cdot}2H2O]_2$ for which an EPR spectrum was observed despite magnetic and optical measurements indicated a singlet ground state: this was attributed either to defective sites or to the effect of residual solvent molecules in the lattice.[29] The XRPD pattern (Fig. S12) gave no evidence of the presence of other crystalline phases, so that the species responsible for the EPR signal is less than 5%.

Concluding, we studied the magnetic anisotropy of three derivatives of the LnTRENSAL family using CTM. The set of CF parameters used to correctly reproduce these data provided an energy pattern different from the one extracted by luminescence measurements, especially in the case of **Tb** and **Dy**, for which no direct luminescence information was available for their ground multiplet. The use of torque magnetometry can efficiently flank spectroscopic techniques to model the magnetic anisotropy of lanthanide based SMMs.

ASSOCIATED CONTENT

Supporting Information

Experimental details, crystal orientations and reference frames, torque curves and fits, XRPD patterns, EPR spectra and composition of the states. This material is available free of charge via the Internet at http://pubs.acs.org.

AUTHOR INFORMATION

Corresponding Author

*E-mail: roberta.sessoli@unifi.it

ACKNOWLEDGMENTS

We acknowledge the financial support of EC through ERC-AdG MolNanoMas (267746) and of MIUR through the project Futuro in Ricerca 2012 (RBFR12RPD1).

REFERENCES

1. Gatteschi, D.; Sessoli, R.; Villain, J., *Molecular nanomagnets*. Oxford University Press: Oxford, UK, **2006**, 1-13.
2. Ishikawa, N., *Polyhedron* **2007,** *26*, 2147-2153.
3. Jiang, S.-D.; Liu, S.-S.; Zhou, L.-N.; Wang, B.-W.; Wang, Z.-M.; Gao, S., *Inorg. Chem.* **2012,** *51*, 3079-3087.
4. Chilton, N. F.; Collison, D.; McInnes, E. J.; Winpenny, R. E.; Soncini, A., *Nat. Commun.* **2013,** *4*.
5. Aravena, D.; Ruiz, E., *Inorg. Chem.* **2013,** *52*, 13770-13778.
6. Baldoví, J. J.; Cardona-Serra, S.; Clemente-Juan, J. M.; Coronado, E.; Gaita-Ariño, A.; Palii, A., *J. Comput. Chem.* **2013,** *34*, 1961-1967.
7. Baldoví, J. J.; Clemente-Juan, J. M.; Coronado, E.; Gaita-Ariño, A.; Palii, A., *J. Comput. Chem.* **2014,** *35*, 1930-1934.
8. Boulon, M. E.; Cucinotta, G.; Luzon, J.; Degl'Innocenti, C.; Perfetti, M.; Bernot, K.; Calvez, G.; Caneschi, A.; Sessoli, R., *Angew. Chem.* **2013,** *125*, 368-372.
9. Cucinotta, G.; Perfetti, M.; Luzon, J.; Etienne, M.; Car, P. E.; Caneschi, A.; Calvez, G.; Bernot, K.; Sessoli, R., *Angew. Chem. Int. Edit.* **2012,** *51*, 1606-1610.
10. Lucaccini, E.; Sorace, L.; Perfetti, M.; Costes, J.-P.; Sessoli, R., *Chem. Commun.* **2014,** 50, 1648-1651.
11. Kanesato, M.; Yokoyama, T.; Itabashi, O.; Suzuki, T. M.; Shiro, M., *Bull. Chem. Soc. Jpn.* **1996,** *69*, 1297-1302.
12. Bernhardt, P. V.; Flanagan, B. M.; Riley, M. J., *Aust. J. Chem.* **2000,** *53*, 229-231.
13. Dreiser, J.; Wäckerlin, C.; Ali, M. E.; Piamonteze, C.; Donati, F.; Singha, A.; Pedersen, K. S.; Rusponi, S.; Bendix, J.; Oppeneer, P. M., *ACS Nano* **2014**.
14. Pedersen, K. S.; Ungur, L.; Sigrist, M.; Sundt, A.; Schau-Magnussen, M.; Vieru, V.; Mutka, H.; Rols, S.; Weihe, H.; Waldmann, O., *Chem. Sci.* **2014,** 5, 1650-1660.
15. Flanagan, B. M.; Bernhardt, P. V.; Krausz, E. R.; Lüthi, S. R.; Riley, M. J., *Inorg. Chem.* **2002,** *41*, 5024-5033.
16. Flanagan, B. M.; Bernhardt, P. V.; Krausz, E. R.; Lüthi, S. R.; Riley, M. J., *Inorg. Chem.* **2001,** *40*, 5401-5407.
17. Perfetti, M.; Cucinotta, G.; Boulon, M. E.; El Hallak, F.; Gao, S.; Sessoli, R., *Chem. Eur. J.* **2014,** *20*, 14051-14056.
18. Kuz'min, M., *J. Magn. Magn. Mater.* **1996,** *154*, 333-338.
19. Cornia, A.; Gatteschi, D.; Sessoli, R., *Coord. Chem. Rev.* **2001,** *219*, 573-604.
20. Godin, M.; Tabard-Cossa, V.; Miyahara, Y.; Monga, T.; Williams, P.; Beaulieu, L.; Lennox, R. B.; Grutter, P., *Nanotechnology* **2010,** *21*, 075501.
21. Cornia, A.; Affronte, M.; Jansen, A. G. M.; Gatteschi, D.; Caneschi, A.; Sessoli, R., *Chem. Phys. Lett.* **2000,** *322*, 477-482.
22. Cornia, A.; Affronte, M.; Jansen, A. G. M.; Abbati, G. L.; Gatteschi, D., *Angew. Chem. Int. Ed.* **1999,** *38*, 2264-2266.
23. Rigamonti, L.; Cornia, A.; Nava, A.; Perfetti, M.; Boulon, M.-E.; Barra, A.-L.; Zhong, X.; Park, K.; Sessoli, R., *PCCP* **2014**.
24. Cornia, A.; Jansen, A. G. M.; Affronte, M., *Phys. Rev. B* **1999,** *60*, 12177-12183.
25. Sievers, J., *Z. Phys. B: Condens. Matter* **1982,** *45*, 289-296.
26. Rinehart, J. D.; Long, J. R., *Chem. Sci.* **2011,** *2*, 2078-2085.
27. Görller-Walrand, C.; Binnemans, K., *Handbook of Physics and Chemistry of Rare Earths* **1996,** *23*, 121-283.
28. Marx, R.; Moro, F.; Dörfel, M.; Ungur, L.; Waters, M.; Jiang, S.; Orlita, M.; Taylor, J.; Frey, W.; Chibotaru, L., *Chemical Science* **2014,** 5, 3287-3293.
29. Baker, J.; Hutchison, C.; Leask, M.; Martineau, P.; Robinson, M., *Proc. R. Soc. Lond. A.* **1987,** *413*, 515-528.

Table of Contents Synopsis

Torque magnetometry based on capacitive cantilevers appears to be very well suited to investigate the magnetic anisotropy of lanthanide ions, which is currently a hot topic in molecular magnetism. Single crystals of trigonal complexes of late lanthanides with the anion of the 2,2’,2’’-tris(salicylideneimino)trimethylamine have been investigated with this technique and the results, modelled with a Crystal Field approach, have evidenced sizeable discrepancies from previously reported data based on luminescence spectra.